water

MDPI

Article

Phytoplankton Community Diversity and Its Environmental Driving Factors in the Northern South China Sea

Wenqing Chen [1,†], Jie Gao [1,†], Zongjun Xu [2,†], Yantao Yan [1] and Shimin Yang [1,*]

[1] College of Marine Life Sciences, Ocean University of China, Qingdao 266003, China
[2] MNR Key Laboratory of Marine Eco-Environmental Science and Technology, First Institute of Oceanography, Ministry of Natural Resources, Qingdao 266061, China
* Correspondence: yangshimin@ouc.edu.cn
† These authors contributed equally to this work.

Abstract: The South China Sea (SCS) plays an important role in global marine ecology. Studies of phytoplankton diversity promote the sustainable utilization of resources in the SCS. From July to August 2020, the phytoplankton community structure at 47 stations in the northern SCS was investigated. Species composition and distribution of phytoplankton, water quality, diversity index, main influencing factors, and succession characteristics of the community structure were analyzed in combination with the survey results from previous years. A total of 332 separate taxa from 83 genera and three phyla were identified, including 142 species and 45 genera of Bacillariophyta, 188 species and 36 genera of Dinophyta, and two species and two genera of Chrysophyta. Average phytoplankton cell abundance was 649.97 cells/L. *Nitzschia* spp., *Thalassionema nitzschioides*, and *Scrippsiella* spp. were the dominant species. *Scrippsiella* spp. was found for the first time as a dominant species in the northern SCS. Meanwhile, *Nitzschia* spp. was associated with organic-polluted water. The high-value areas of *Nitzschia* spp. also indicated eutrophication, and water was slightly polluted. The Shannon–Weiner diversity index of the surface layer was 0.99–4.56 (with a mean of 3.57), and the evenness index was 0.23–0.96 (with a mean of 0.83). The phytoplankton community structure in the northern SCS was deemed to be stable. Pearson correlation analysis showed that the sum of nitrate and nitrite was significantly negatively correlated with the abundance of dinoflagellate, which indicated restrictions as a result of the sum of nitrate and nitrite, with no significant correlation between ammonium salt and various groups. Small- and medium-sized phytoplankton are usually dominant in the SCS, where nitrogen is limited.

Keywords: northern South China Sea; phytoplankton; community structure; environmental factor; eutrophication; diversity

Citation: Chen, W.; Gao, J.; Xu, Z.; Yan, Y.; Yang, S. Phytoplankton Community Diversity and Its Environmental Driving Factors in the Northern South China Sea. *Water* **2022**, *14*, 3777. https://doi.org/10.3390/w14223777

Academic Editor: Jun Yang

Received: 27 October 2022
Accepted: 17 November 2022
Published: 21 November 2022

1. Introduction

Phytoplankton are the most crucial primary producers in the ocean, accounting for approximately 95% of the primary productivity of the ocean [1,2] and approximately half of the global net primary productivity [3]. Phytoplankton convert inorganic matter into organic matter through photosynthesis and promote the absorption of nutrients dissolved in seawater above the euphotic layer, which introduces energy and substances into the food chain and transfers them to a higher trophic level that opens a series of marine food webs [2,4]. The active vertical movement of phytoplankton is critical for carbon storage and flux, as well as marine biological resources [5]. Environmental factors have had a dynamic impact on biological communities. Changes in physical and chemical factors in the ocean can directly influence the physiological characteristics of phytoplankton [6], thereby altering their community structure [7]. Therefore, by studying the changes in phytoplankton community structure, we can understand the environmental changes in the local sea area better, which is of great significance in the study of marine ecology.

The South China Sea (SCS) is one of three marginal seas in China. It has a monsoon climate that includes tropical and subtropical climatic zones. The northern SCS is connected to the East China Sea in the north and is affected by Pacific water in the east, while the continental shelf in the west is greatly affected by land sources. The Pearl River and other rivers carry large amounts of nutrients and other substances from their estuaries. During the summer, the northern SCS is affected by the interactions between circulation, coastal currents, and upwelling in the SCS [8]. In addition, the internal waves in the northern SCS are the largest reported in the global ocean [9]. Many ocean currents cause seasonal changes in the phytoplankton community structure.

The water quality directly affects the abundance, community structure and diversity of phytoplankton. Human activities, such as the rapid development of tourism and sewage discharge, can all contribute to poor water quality, which endangers the health of the ecosystem [10,11]. Eutrophication is a typical example, which is usually caused by hypoxia and an increasein the number of algae [12]. At present, eutrophication has become a global problem, which has brought serious negative impacts to the marine ecosystem.

Previous studies of the South China Sea have focused on coastal bays or aquaculture waters, and less attention has been paid to the large surface stations in the northern SCS. Few studies have evaluated the water quality in the northern SCS. In this study, based on an analysis of water-collected phytoplankton samples from 47 large surface stations in the northern SCS, the species composition, cell abundance, dominant population, and diversity index of phytoplankton were systematically studied in order to clarify the diversity of phytoplankton in the SCS and reflect the eutrophication of the sea area. Based on this, the water quality of the investigated area was analyzed. In comparison with historical data, we discussed the changes in the phytoplankton composition in the northern SCS in recent years. Simultaneously, ecological statistics were used to correlate the phytoplankton with environmental factors, and the environmental factors driving the change in phytoplankton community structure were discussed. This study provides a basis for studying the response of the phytoplankton community structure in the northern SCS to global environmental changes and human activities on a large temporal scale, and it assessed water quality in the northern SCS with the aim of better introducing relevant measures for management.

2. Materials and Methods

From 19 July to 10 August 2020, 47 stations were investigated in the northern SCS (15–22° N, 114–120° E) (Figure 1) and 270 bottles of samples were collected in total. Approximately 2000 mL of water samples were collected at water depths of 0 (surface), 30, 50, 75, 100, and 150 m using a Conductivity Temperature Depth water sampler mounted on a Seabird 911 Plus CTD (Seabird Electronics Inc., Bellevue, WA, USA). Among them, the S1 station only collected samples at water depths of 0 and 30 m, the S2 station collected samples at 0, 30 and 50 m, samples with water depths of 75 m and above were collected at the S3 and S4 stations, and the samples at 150 m were collected at the S5 station. Then, 2% Lugol's iodine solution was added to the water samples for fixation. In the laboratory, we concentrated 2000 mL samples to X mL samples, respectively (the range of X is 100–300), so that we could classify and identify phytoplankton more easily. We evenly took out B mL samples from X mL samples and poured them into a Hydro-Bio counting chamber (Hydro-Bios; Kiel, Germany) for 24 h. The magnification of the microscope eyepiece was 10× and the microscope objective was 20× or 40×. The total magnification was 200× or 400×. The Utermöhl method was used to analyze the phytoplankton [13–15]. Phytoplankton cells were counted and identified using a Nikon TS100 inverted microscope (Nikon Corporation of Japan, Tokyo, Japan), and we consulted relevant books for their identification [16–19].

Temperature, salinity, and nutrient data (NH4-N, NO2-N, NO3-N, PO4-P, and SiO3) were obtained from the First Institute of Oceanography, and were determined by the SEAL-AA3 Auto Continuous Flow Analytical System. Wherein, NO3-N and NO2-N adopted the diazotization-coupling method (NO3-N Zn-Cd reduction); NH4-N, PO4-P and SiO3 used

the sodium salicylate method, phosphorus molybdenum blue method, and silicomolybdic blue method, respectively.

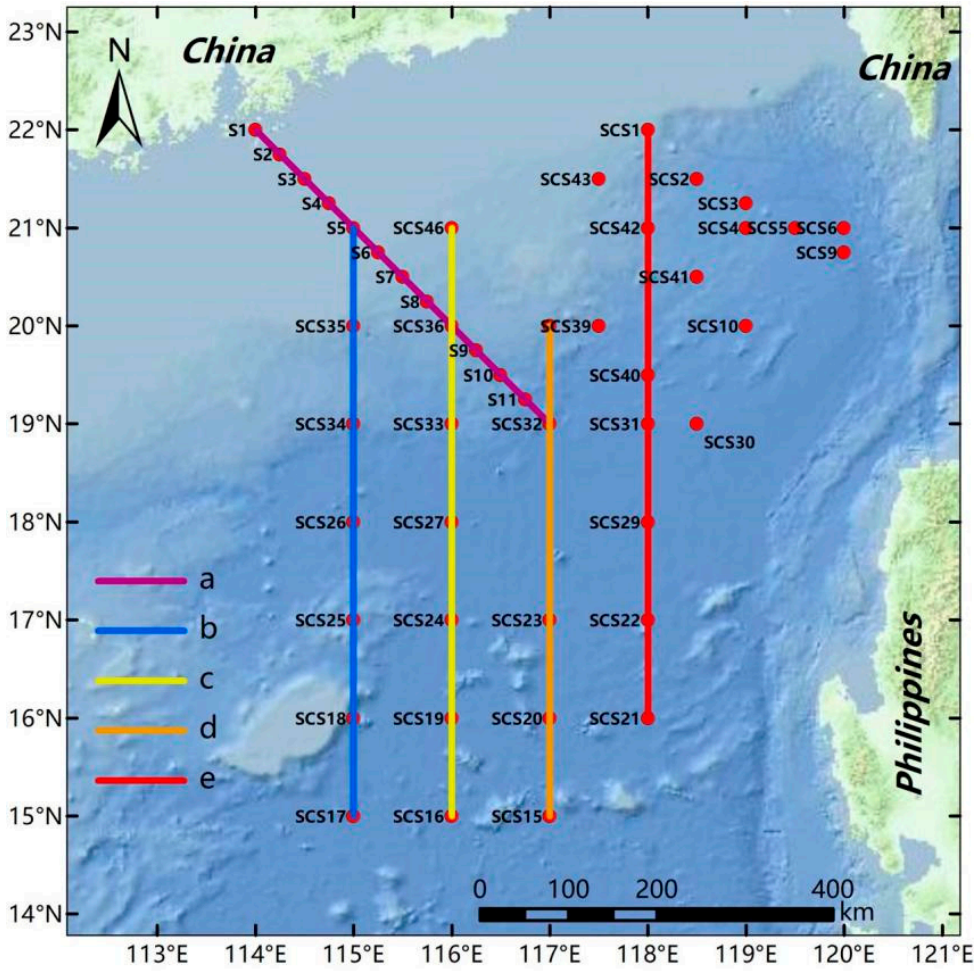

Figure 1. Locations of the sampling stations in the northern South China Sea.

The calculation formula of phytoplankton abundance was as follows [14,15]:

$$\text{Phytoplankton abundance} = \frac{A}{B} * \frac{X}{2} \text{ cells/L}$$

where, A is the quantity of certain phytoplankton in the Hydro-Bio counting chamber, B is the volume of the sample in the Hydro-Bio counting chamber, and X is the volume after concentration.

The Shannon–Wiener index (H') [20] was used to determine phytoplankton biodiversity, and was calculated as:

$$H' = -\sum_{i=1}^{S} Pi \log_2 Pi \quad (1)$$

The evenness of the phytoplankton samples was calculated by Pielou's index (J') [21]:

$$J = H' / \log_2 S \quad (2)$$

The dominance index (Y) was used to determine the dominant species, where $Y > 0.02$ indicated the dominant species [22]:

$$Y = n_i / N \times f_i \quad (3)$$

Pi shows the significance probability for all species. Where $Pi = ni/N$, *ni* is the number of individuals of the *i*th species, *N* is the total number of phytoplankton cells, *S* is the number of identified species in a sample, and f_i is the frequency of occurrence of the *i*th species in each sample.

We used R software (version: 4.2.0) to analyze the relationship between variables and the strength of the relationship and visualized the results. We used Primer software (Primer 6) to do hierarchical clustering and made comparisons of the clusters with ANOVA. Surfer software (version: 26.0) was used to draw plane and section distribution maps, and ArcGis (version: 10.2) was used to draw the map of sampling stations.

3. Results

3.1. Environment of the Investigated Sea Area in the Northern South China Sea

The plane distribution of temperature (Figure 2a) and salinity (Figure 2b) in the investigated sea area is shown in Figure 2. The temperature varied from 15.4 °C to 31.9 °C, with an average of 25.1 °C. The salinity was 31.91–34.69, with an average of 34.32. In general, the temperature decreased with the depth, and the salinity distribution was relatively uniform There was little difference among water layers.

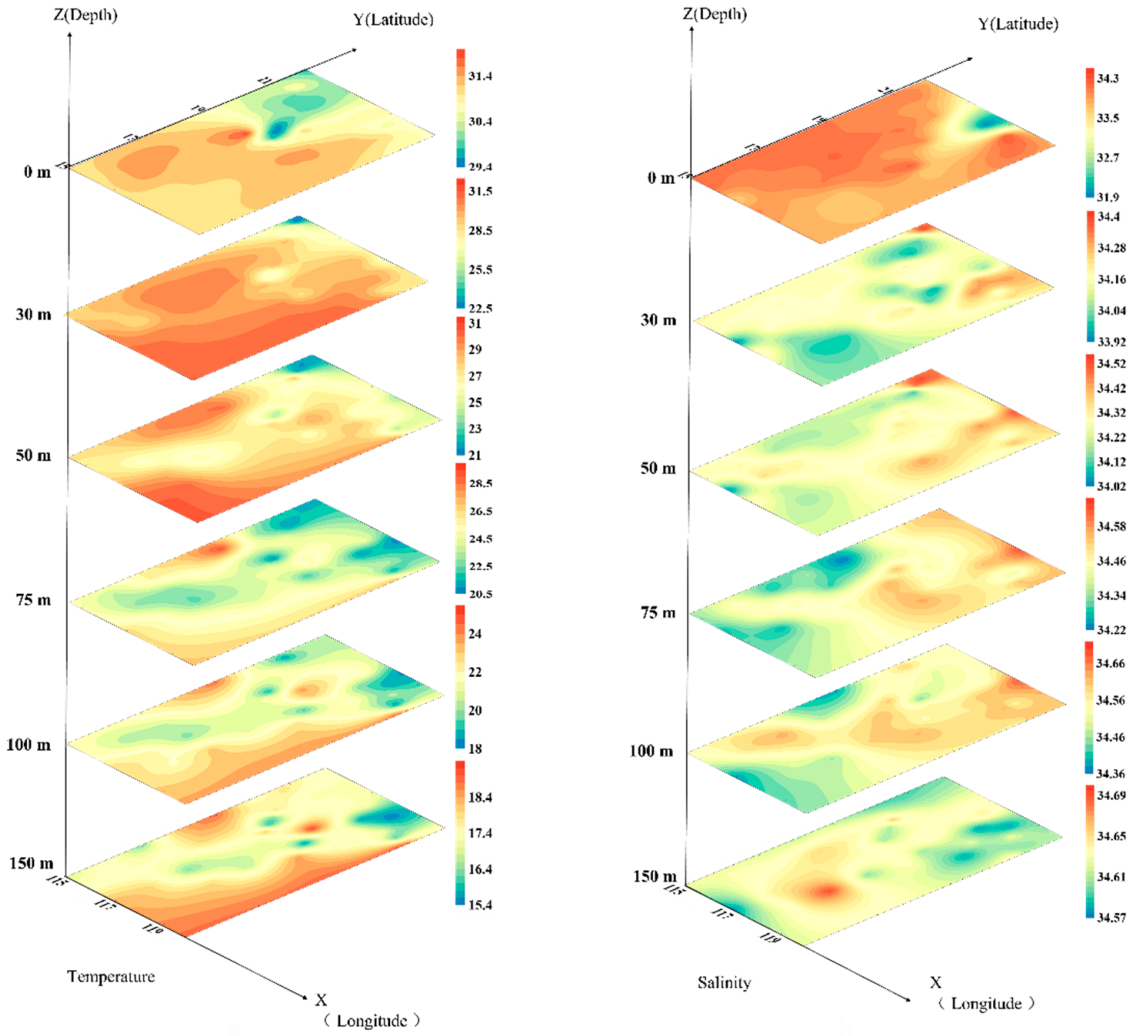

Figure 2. The temperature and salinity in the six water layers at sampling stations in the northern South China Sea.

3.2. Species Composition, Cell Abundance, and Ecological Type of Phytoplankton

A total of 332 species (including varieties and forms) belonging to 83 genera in three phyla were identified (Appendix A). Among these, 142 species and 45 genera of Bacillariophyta were identified, accounting for 42.77% of the total species. The main genus of Bacillariophyta was *Chaetoceros* spp., accounting for 39 species and 27.46% of the diatom species. There were 188 species belonging to 36 genera in Dinophyta, accounting for 56.63% of the total species. Among them, 33 were *Neoceratium* spp., accounting for 17.55% of the total dinoflagellate species. There were 29 species of *Protoperidinium* spp., accounting for 15.43% of the total. In addition, two species from the two Chrysophyta accounted for 0.60%of the total species. *Ceratocorys horrida* and *Ornithocercus steinii* were also found northeast of the survey area. These oceanic species are widely distributed from the warm temperate zone to the tropical ocean and the Kuroshio area of the East China Sea. Therefore, they can be used as indicator species for the Kuroshio invasion [23].

The total abundance of phytoplankton in the survey area was 0.38×10^5–400.24×10^5 cells/L, with an average of 6.50×10^5 cells/L. Diatom abundance was 0.03×10^5–92.55×10^5 cells/L, with an average of 5.33×10^5 cells/L, accounting for 82.03% of the total cell abundance, which indicated dominance. Dinoflagellate abundance was 0.04×10^5–8.02×10^5 cells/L, with an average of 1.15×10^5 cells/L, accounting for 17.66% of the total cell abundance. The average cell abundance of Chrysophyceae was 0.02×10^5 cells/L, accounting for 0.31% of the total cell abundance. The ecological types of phytoplankton in this survey were mainly eurythermic and widespread species, such as *Nitzschia* spp. and *Thalassionema nitzschioides*, as well as coastal and warm-water species, such as *Pseudo-nitzschia delicatissima* and *Chaetoceros constrictus*, and the distribution of offshore species was low.

3.3. Plane Distribution of Phytoplankton

The plane distribution of phytoplankton in each water layer in the investigated sea area is shown in Figure 3. The layers with the highest cell abundance of phytoplankton(Figure 3a), diatoms(Figure 3b), and dinoflagellates(Figure 3c) were 30, 30, and 50 m, respectively. In the surface layer, the abundance of phytoplankton cells was 62–4066 cells/L, with an average of 512 cells/L. Most of the areas with high phytoplankton cell abundance were located at the SCS43 station in the north of the survey area and the S1 station near the coast of Guangdong. Overall, the distribution gradually decreased from north to south and from west to east. The cell abundance of diatoms was 3–9255 cells/L, with an average of 352 cells/L. Cell abundance reached its highest value in the north of the survey area and gradually decreased from north to south. The abundance of dinoflagellates was 30–331 cells/L, with an average of 159 cells/L. The highest value was at the S2 station near the coast of Guangdong, and the abundance of *Scrippsiella* spp. was high. In general, dinoflagellate abundance was distributed in patches.

The total abundance of phytoplankton in the 30 m layer was 73–40,024 cells/L. The highest phytoplankton cell abundance in this survey was 40,024 cells/L at the S1 station, and the abundance of *Nitzschia* spp. was high. The average phytoplankton cell abundance at stations other than S1 was 482 cells/L. The cell abundance of diatoms in the 30 m layer was 15–397,552 cells/L, reaching the highest value of 39,752 cells/L at the S1 station near the shore. The average diatom cell abundance at all stations (except S1) was 297 cells/L. The highest abundance of dinoflagellates was 27–494 cells/L at in the 50 m layer, with an average of 155 cells/L. At the SCS19 station in the south of the survey area, a high-value area was found, which was jointly distributed by *Scrippsiella* spp. and *Gyrodinium* spp., and showed a distribution of low abundance in the north and south, and a higher abundance in the east than in the west.

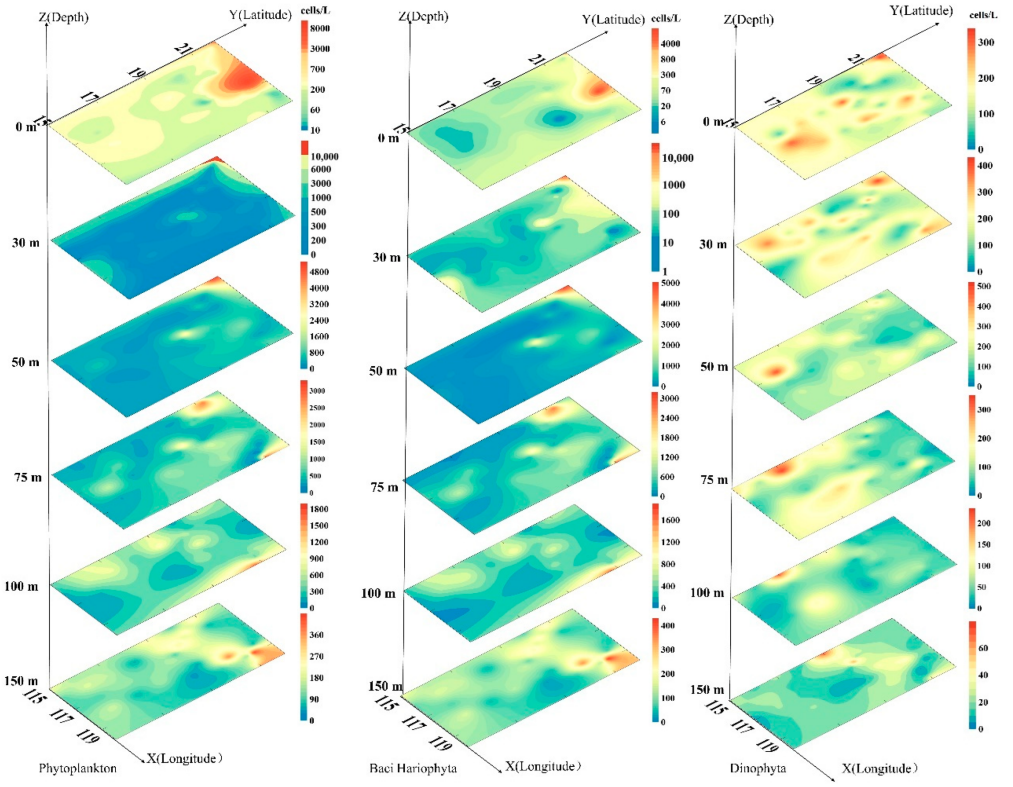

Figure 3. The cell abundance of total phytoplankton, diatoms, and dinoflagellates in the six water layers at sampling stations in the northern South China Sea.

3.4. Vertical Distribution of Phytoplankton

As seen in Figure 1, the survey was divided into four longitudinal sections and one section from northwest to southeast. Figure 4 shows the distribution of phytoplankton in each section. In Section A, the distribution of phytoplankton and diatoms was consistent. The maximum cell abundance in this survey appeared at the 30 m layer of the S1 station near the shore, and the dominant species was *Nitzschia*. The diatom cell abundance was concentrated nearshore, mainly in the 30 m and 50 m layers, while offshore, it was mostly in the 50 m and 75 m layers. The distribution of cell abundance decreased from coastal to offshore areas, which is consistent with the distribution of nutrients. The patch distribution of dinoflagellates was obvious and was mainly distributed in the water above the 75 m layer.

Sections B, C, D, and E are four north–south sections arranged in parallel from west to east. Diatoms accounted for a large proportion of the total abundance of phytoplankton; therefore, the distribution of phytoplankton was similar to that of diatoms. The high abundance of phytoplankton and diatom cells in Section B was mainly located at the 75 m water layer of the S5 station near the shore, and the dominant species was C. curvisetus. The high diatom cell abundance area was mainly located in the 100 m layer, and dinoflagellates were densely distributed offshore. In Section C, the patch distribution of phytoplankton and diatoms was clear, and high-value areas appeared from the nearshore to the far sea. The distribution of phytoplankton and diatoms in Section D first increased and then decreased with the increase in water depth. The 30 m layer of the SCS15 station in the south of the survey area had the greatest abundance, with many *Nitzschia* spp. and C. curvisetus. Dinoflagellates were distributed in high-abundance areas from the nearshore to the far sea, and most were located above the 75 m layer. In Section E, the abundance of phytoplankton in the north was higher than that in the south. The high-value area of diatoms was mainly distributed in the 50 m layer, while dinoflagellates often appeared in the high-value area on the surface. Generally, areas with a high abundance of phytoplankton cells were distributed

in the 30 m layer near the shore, whereas those in the open sea were mainly concentrated in the 75 m layer.

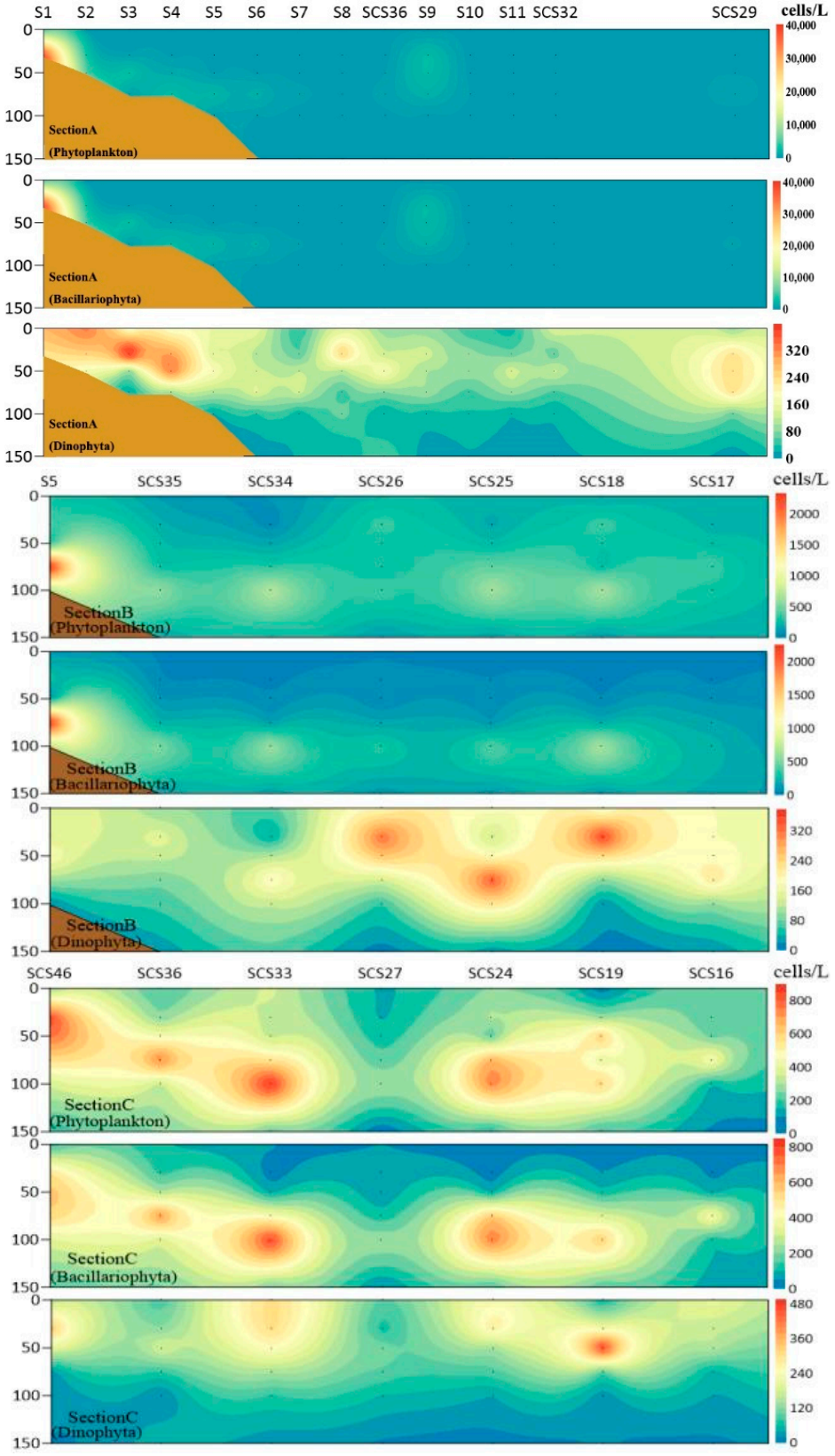

Figure 4. *Cont.*

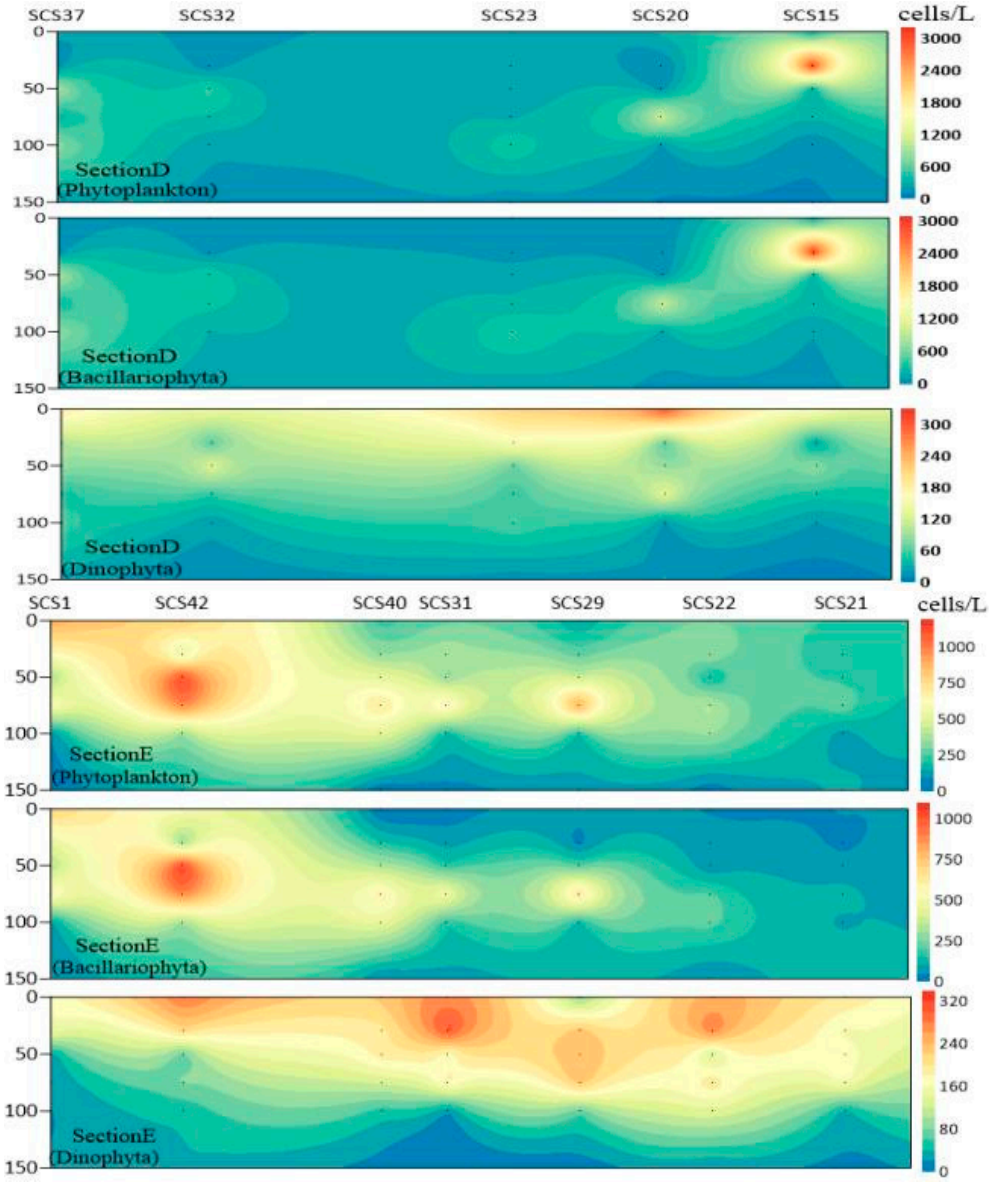

Figure 4. Vertical distribution of cell abundance in Transects A, B, C, D, and E in the northern South China Sea.

3.5. Dominant Species of Phytoplankton and Their Horizontal Distribution

Nitzschia spp., *Thalassionema nitzschioides*, and *Scrippsiella* spp. were the dominant phytoplankton species in the northern SCS during the summer. *Nitzschia* spp. was the dominant species in this survey, with a frequency of 94.4%. *Scrippsiella* spp. was the only dominant dinoflagellate species with a frequency of 68.1%, second only to *Nitzschia* spp. (Figure 5). The high-value area of *Nitzschia* spp. (Figure 5a) in the surface layer was mainly located at the S1 station near the shore and the SCS43 station near the intersection of the Taiwan Strait and SCS. *Nitzschia* spp. appeared less frequently in the south and northeast regions of the survey area. The *Nitzschia* spp. in the 30 m layer were mostly distributed near the S1 station, where the highest abundance of *Nitzschia* spp. cells in this survey was 26,313 cells/L. Overall, cell abundance showed a decreasing trend from the S1 station to the surroundings, with a high value at the SCS15 station in the south. The high-abundance area of *Thalassionema nitzschioides* (Figure 5b) in the surface layer was located at stations S1 and S2 near the shore and decreased to the east and south of the investigation area. The cell abundance of *Thalassionema nitzschioides* was the highest in the 30 m layer, and the

high-value areas were mostly concentrated near the shore, whereas their distribution in the open sea was lower. This indicates cold and warm changes in paleotemperature in the northern SCS [24]. The area with a high abundance of *Scrippsiella* spp. (Figure 5c) in the 0 m water layer was mainly located near the shore and in the middle of the survey area. The abundance was highest in the 50 m layer, and appeared more frequently in the southwestern part of the survey area. In general, cell abundance in the southern sites was higher than that in the northern sites.

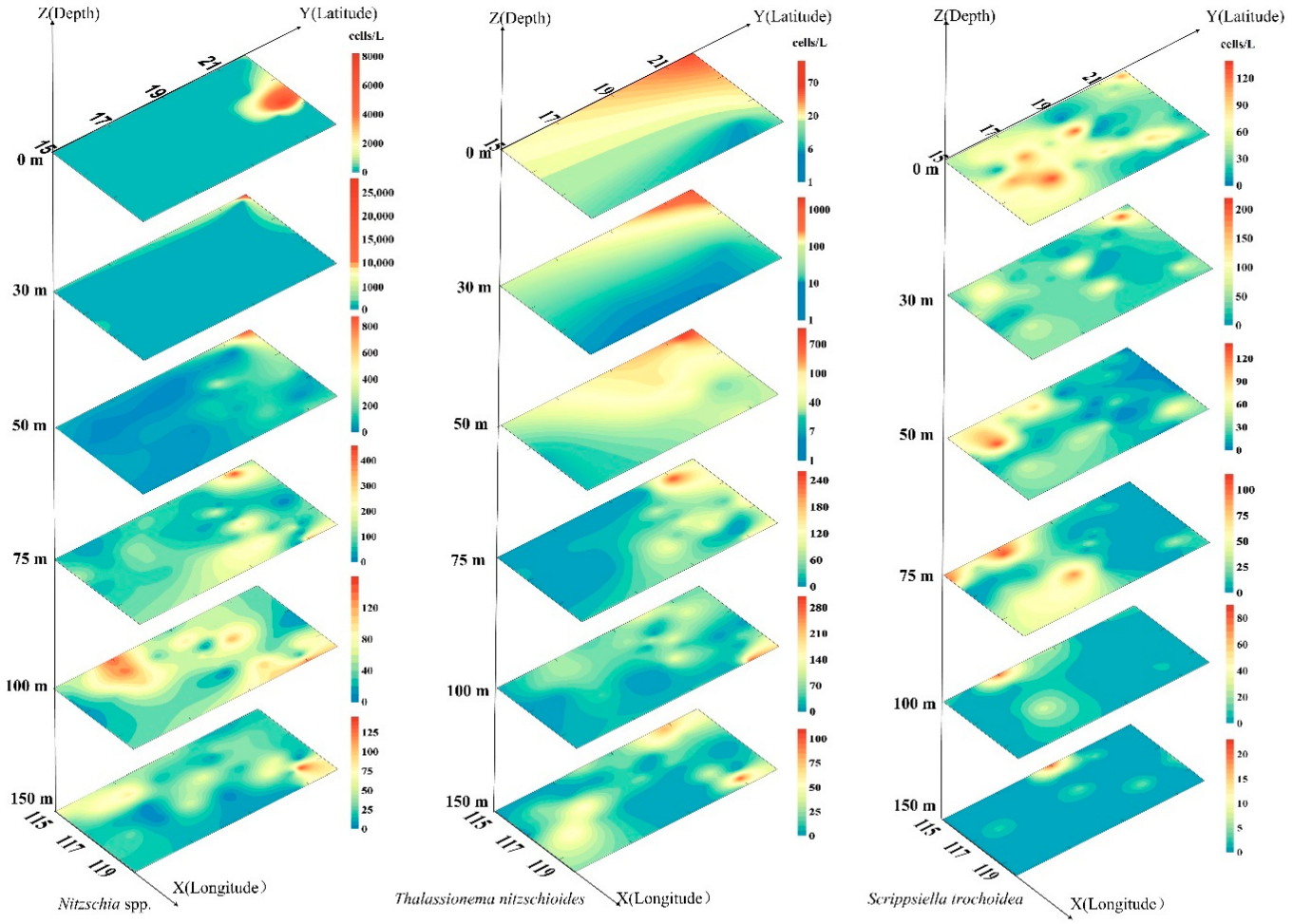

Figure 5. Horizontal distribution of the most dominant species in the sampling stations in the northern South China Sea.

3.6. Diversity and Evenness Index of the Phytoplankton Community

Shannon–Wiener diversity (Figure 6a) and Pielou evenness indices (Figure 6b) were used to measure the stability of the phytoplankton community structure. The Shannon–Weiner diversity index of surface phytoplankton in the investigated sea area was 0.99–4.56, with an average of 3.57, and the evenness index was 0.23–0.96, with an average of 0.83. The average value of the diversity and evenness indices was the highest in the 75 m layer, whereas the Shannon–Weiner diversity index was 3.08–5.02, with an average of 4.39, and the evenness index was 0.72–0.93, with an average of 0.85.

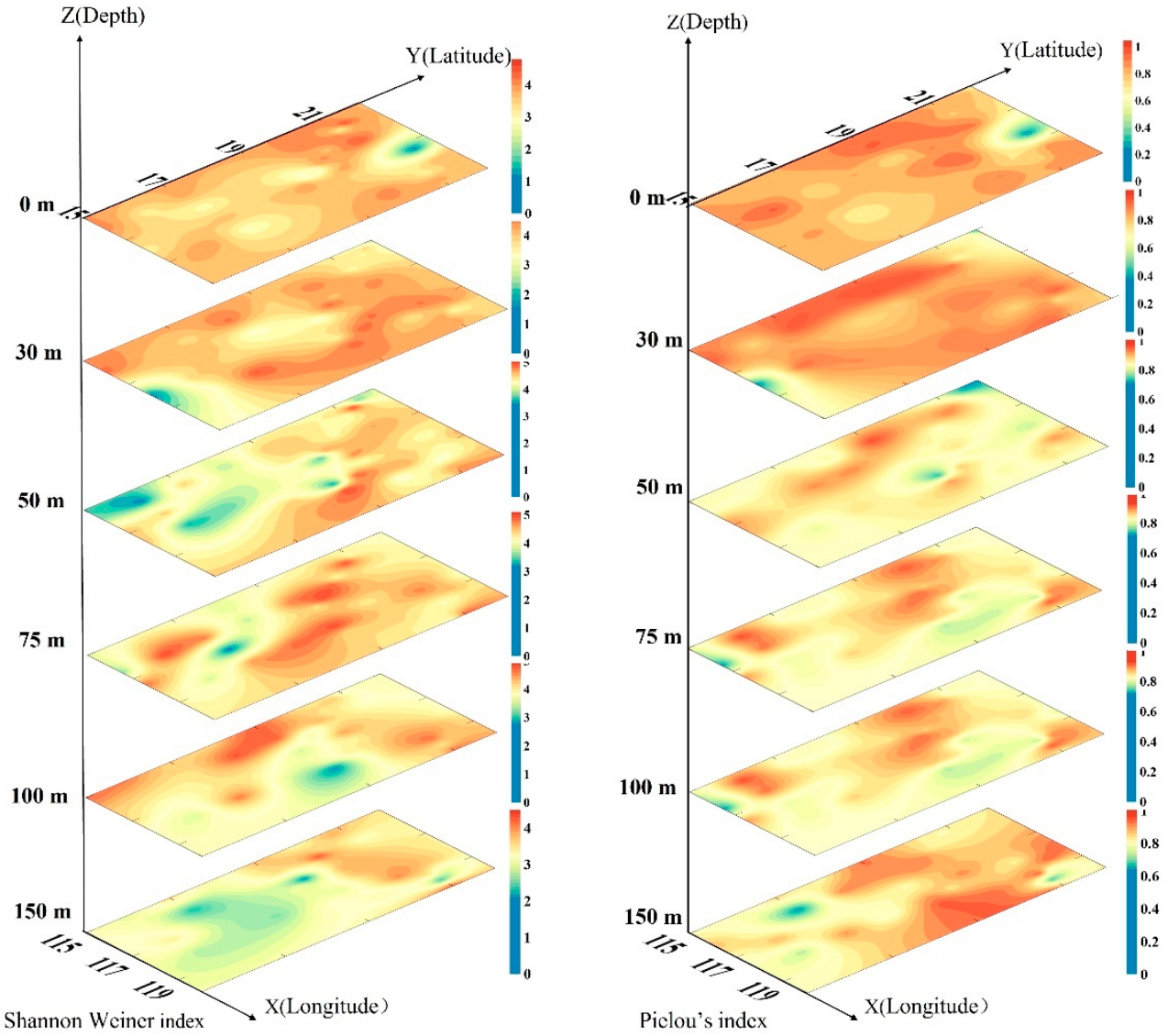

Figure 6. Shannon Weiner and Pielou indices in the six layers of sampling stations in the northern South China Sea.

3.7. Correlation Results

The cell abundance of phytoplankton, diatoms, dinoflagellates, and dominant species were combined with environmental factors (temperature, salinity, phosphate, silicate, ammonium salt, nitrate, and nitrite) for Pearson correlation analysis (Figure 7). The abundance of dinoflagellate cells was positively correlated with temperature, which is consistent with the preference of dinoflagellates for high-temperature living environments. Additionally, the abundance of dinoflagellate cells was negatively correlated with salinity, depth, silicate, phosphate, and the sum of nitrate and nitrite levels. In general, phytoplankton and diatoms did not show a certain correlation with these environmental factors. Among the dominant species, *Scrippsiella* spp. had a significant negative correlation with temperature, and *Nitzschia* spp. were greatly affected by salinity. As with the phytoplankton and diatoms, *Thalassionema nitzschioides* had no correlation with environmental factors. Ammonium salt had little effect on phytoplankton in the northern SCS. Contrary to other nutrients, ammonium salt was positively correlated with depth and negatively correlated with salinity.

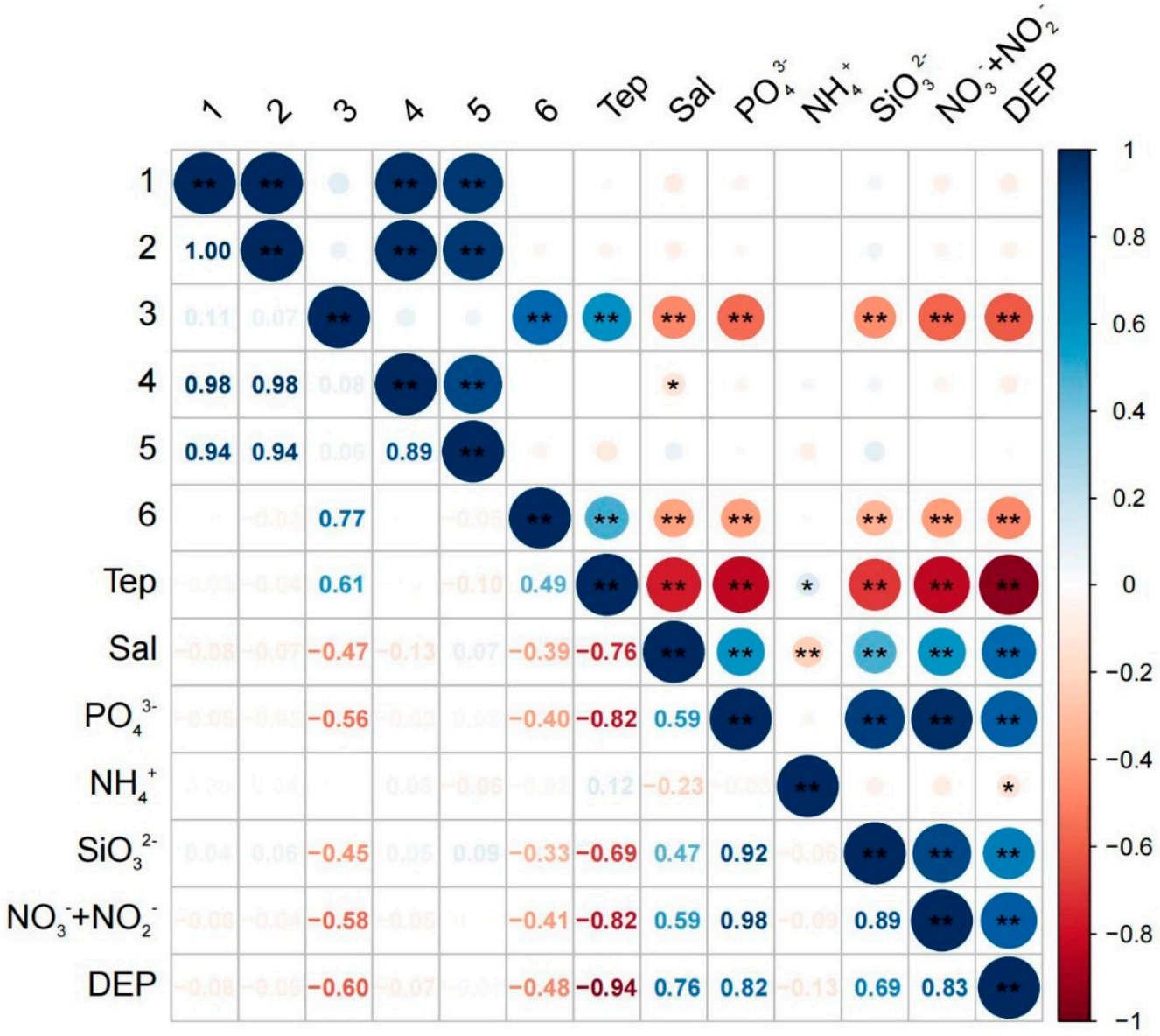

Figure 7. Pearson analysis between phytoplankton and environmental factors. 1, phytoplankton; 2, diatom; 3, dinoflagellate; 4, *Nitzschia* sp.; 5, *Thalassionema nitzschioides;* 6, *Scrippsiella trochoidea;* DEP, depth; Tep, temperature; Sal, salinity; PO_4^{3-}, phosphate; SiO_3^{2-}, silicate; NH_4^+, ammonium salt; NO_2^-, nitrite; NO_3^-, nitrate.

3.8. Cluster Analysis of Community Structure

Hierarchical cluster analysis was conducted for each station according to the species and cell abundance of each station (Figure 8). The results showed that the Bray–Curties similarity coefficient between the largest stations was mostly 40–60% in each layer. In the surface, 47 stations were divided into two groups. S1, SCS43, and SCS1 stations, which were located in the north of SCS, were divided into group I. The other stations were divided into group II. The average cell abundance of phytoplankton in group I was 4774 cells/L, which was much higher than that in the group II (221 cells/L). Some nearshore species, such as *skeletonema costatum*, mostly occurred in group 1, and group II mainly consisted of widespread species and warm-water species. Cluster analysis divided the stations according to their close geographical locations, which indicated that the physical environment was consistent with the biological data.

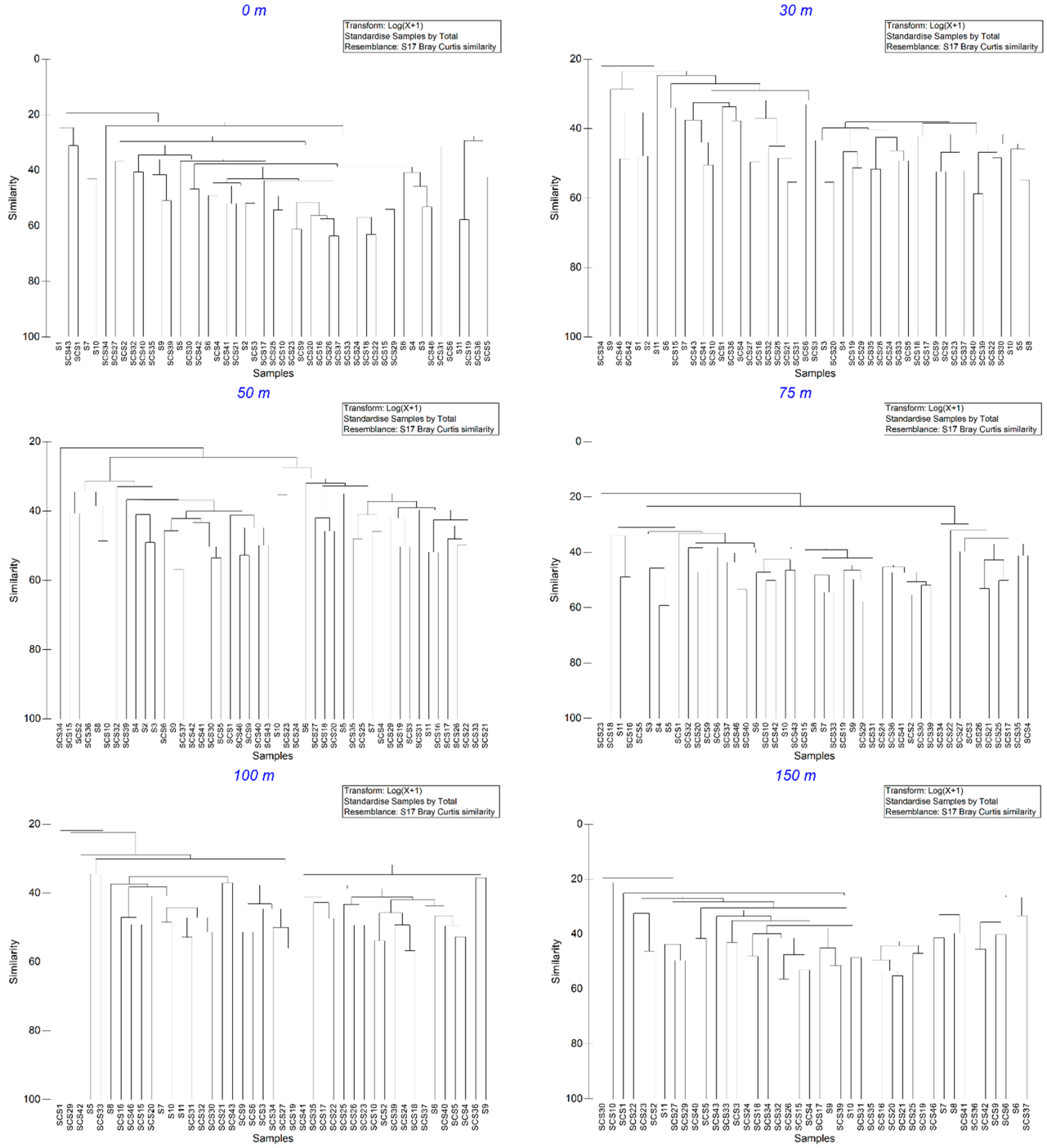

Figure 8. Hierarchical cluster analysis of phytoplankton community structure.

From the perspective of vertical structure, 30 m and 50 m water layers were relatively similar, and the SCS34 station formed an independent group. It indicated that the environment of the two layers might be similar.

4. Discussion

4.1. Factors Affecting the Distribution of Phytoplankton

In the surface layer, the cell abundance distributions of phytoplankton and diatoms were similar, and most areas with high phytoplankton density were located near the Taiwan Strait. This area is on the east coast of Guangdong, and is greatly affected by freshwater and land-based inputs from the Pearl River. In addition, this area is jointly influenced by the

coastal current of Guangdong, summer upwelling, the SCS warm current, and the Kuroshio intrusion current in the summer [25,26], making the nutrient content in the north higher than in the south. The cell abundance of diatoms gradually decreased from north to south, which is consistent with their preference for high-nutrient environments [27]. At the 30 m layer, the highest abundance of phytoplankton and diatom cells in this survey appeared at the S1 station near the coast of Guangdong, where *Nitzschia* spp. were the dominant species. As the area was affected by freshwater in the Pearl River estuary, the high-abundance area of phytoplankton usually did not appear in the surface water. Instead, it was between the surface and bottom fronts of freshwater and above the vertical pycnocline [28]. Therefore, the 30 m layer may be the location of the pycnocline.

Generally, areas with a high abundance of phytoplankton cells were distributed in the 30 m layer near the shore, whereas those in the open sea were mainly concentrated in the 75 m layer. However, at stations SCS33 and SCS24 in the middle of the survey area, a high-abundance area appeared at the 100 m layer, which may have been due to the high intensity of the current in the sea area, which transports phytoplankton from the upper to the deeper water [25]. A previous study found that the pycnocline in the north of the site was located at a depth of 60–120 m and that the stratification was strong [29], which is consistent with the observation that the high-value area of phytoplankton in the northern SCS often appeared in the 75 m layer in the current study.

The patch distribution of the dinoflagellates was determined based on their physiological characteristics. Many dinoflagellates are heterotrophic organisms that can obtain organic phosphorus by feeding on diatoms, cyanobacteria, and bacteria [30,31]. They are highly competitive in environments with low nutrient concentrations in the open sea [32,33].

In the surveyed sea area, the maximum value layer of nutrients often appeared at 150 m, whereas the high-value phytoplankton layer often appeared above the 100 m layer. This was mainly due to the exponential attenuation of light in the vertical direction when it propagated in water [34]. Therefore, at 150 m and below, light replaced nutrients as the main limiting factor for phytoplankton growth, resulting in a low abundance of phytoplankton cells.

4.2. Comparison with Historical Data

We found that, at the station near the Pearl River Estuary in the northwest of the investigated sea area, the water temperature was low, and the salinity was high at the 30 m and 50 m water layers, this was contrary to previous studies [35]. This survey was conducted from July to August 2020, when, according to the historical data of the China Meteorological Administration, South China suffered multiple rounds of heavy rainfall during this period. The Pearl River Estuary should have therefore had a large runoff, and the lower water temperature in the coastal waters was likely to be closely related to the increased runoff. Studies showed that upwelling existed in the area from the southern Taiwan Strait to the Pearl River estuary in summer [36]. This may be the reason why the salinity in the north of the survey area was slightly higher.

Table 1 compares the phytoplankton survey results with historical data for the northern SCS. Similar to previous research, diatoms and dinoflagellates were the main communities in the northern SCS, with diatoms being predominant. A total of 332 species were identified in this survey. Based on long-term monitoring results from 2004 to the present, the number of species show a fluctuating upward trend. The cell abundance has fluctuated substantially, and years with high abundance were up to three orders of magnitude worse than years with low abundance. The diversity index showed a fluctuating upward trend over ten years. In addition to investigating the changes in environmental factors in the sea area, with the continuous development of trade globalization, ship transportation has played a major role in the freight market. Ballast water brings a large amount of marine phytoplankton to all parts of the world. In an appropriate environment, some species settle in the sea, resulting in a gradual increase in species diversity [3]. When compared with previous investigations, the composition of the dominant species was different. From 2008 to 2014, *Chaetoceros* spp. often appeared as a dominant species in the northern SCS, but in recent years, it had

gradually lost its dominant position. As a typical oligotrophic area, the SCS was often limited by phosphorus [37]. In order to adapt to the phosphorus deficiency environment, the phytoplankton population will also change. Species with low phosphorus demand and whose phospholipids in cell membranes are easily replaced by lipids containing sulfur or nitrogen will gradually become dominant species [38]. The growth of *Chaetoceros* spp. with high phosphorus demand gradually lost its competitive advantage [39].

Table 1. Comparison of dominant phytoplankton species composition and historical data in the northern South China Sea.

Sampling Data	Survey Area	Sampling Method	Number of Species	Average Cell Abundance (cells/L)	Average Diversity Index	Dominant Species	Reference
August 2020	15°–22° N 114°–120° E	Water sample	332	649.97	3.95	*Nitzschia* spp. *Thalassionema nitzschioides* *Scrippsiella* spp.	This study
May 2015	19°–23.5° N 110.5°–117.5° E	Net sample	378	762.00	3.99	*Rhizosolenia alata* *Thalassiothrix frauenfeldii* *Pseudo-nitzschia pungens* *Eucampia zodiacus* *Nitzschia lorenziana* *Rhizosolenia gracillima*	[40]
August 2014	18°–22° N 114°–116° E	Water sample	229	16318	2.37	*Skeletonema costatum* *Fragilariopsis* spp. *Chaetoceros brevis* *T. nitzschioides* *Pseudo-nitzschia delicatissima* *Pseudo-nitzschia pungens* *Chaetoceros compressus* *Chaetoceros lorenzianus* *Chaetoceros pelagicus*	[35]
August 2012	11°–22° N 110°–116.5° E	Net sample	206	666.70	2.67	*Thalassiothrix frauenfeldii* *Rhizosolenia alata* *Thalassionema T. nitzschioides*	[41]
October 2010~November 2010	18°–23.5° N 110.5°–118° E	Water sample	204	500.00	3.14	*Thalassionema T. nitzschioides* *Navicula* spp. *Skeletonema costatum* *Chaetoceros curvisetus* *Rhizosolenia stolterfothii* *Paralia sulcata*	[42]
August 2009	18°–22° N 110°–117° E	Water sample	109	819.70	—	*Pseudo-nitzschia delicatissima* *Thalassiothrix frauenfeldii* *Pseudo-nitzschia pungens* *Detonula pumila* *Protoperidinium* spp. *Asterionella glacialis*	[43]
August 2008	18°–23° N 110°–120° E	Net sample	169	180.60	—	*Chaetoceros lorenzianus* *Pseudo-nitzschia delicatissima* *Thalassionema T. nitzschioides*	[44]
August 2007	18°–23° N 110°–120° E	Water sample	216	11,220	2.62	*Thalassionema T. nitzschioides* *Thalassiosira* spp. *Skeletonema costatum* *Prorocentrum minimun* *Gymnodinium* spp.	[45]
August 2004–September 2004	18°–22° N 110°–117° E	Water sample	159	115,050	2.08	*Pseudo-nitzschia delicatissima* *Chaetoceros curvisetus* *Chaetoceros diadema* *Prorocentrum dentatum* *Asterionellopsis glacialis* *Thalassionema T. nitzschioides* *Chaetoceros lorenzianus* *Bacteriastrum comosum* *Emiliania huxleyi*	[46]

Widely distributed species such as *Thalassionema* spp. have been dominant for a long time [35,40–46] (Table 1). A typical morphological characteristic of *Thalassionema* spp. is slenderness. This shape increases the surface to volume ratio of the cells and increases the absorption of nutrients. This shape is conducive to the absorption of restricted phosphate, particularly in the oligotrophic sea area of the SCS. *Thalassionema* spp. often appear in clusters, which increases the cell volume and makes them resistant to sinking, so that the population can stay in the euphotic layer for a longer time to accelerate reproduction. When compared to small-sized phytoplankton living alone, phytoplankton living in groups are not easily eaten by zooplankton, which benefits population reproduction [32].

In this investigation, *Scrippsiella* spp., a coastal species, was the only dominant dinoflagellate species, which differed from previous studies. The environmental factors in the northern SCS are complex, and dinoflagellates showed a trend of more species observed, yet in lower quantities; therefore, it was difficult to identify a dominant population. *Scrippsiella* spp. somatic cells are small, and the carbon biomass they convert is relatively low. Because of their flagella and mobility, they suspend more easily in water than diatoms. Therefore, the emergence of *Scrippsiella* spp. as a dominant species may indicate a reduction in carbon flux in the SCS.

4.3. Assessment of Community Structure Stability and Eutrophication in the Northern SCS

The higher the diversity index, the more uniform the distribution of individuals in the community, and the more stable the community. The diversity index of the upper water body was higher than that of the lower water body. Therefore, the community in the upper water body had higher stability. At the surface, an area with low diversity index appeared in the north of the survey area, which was due to the presence of high-density water masses of *Nitzschia* spp. In general, the phytoplankton community structure in the northern SCS was relatively stable and was evenly distributed during the survey period. However, in the northern part of the survey area, the diversity and evenness indices were relatively low because of the massive reproduction of *Nitzschia* spp., and the stability of the community structure was consequently poor. The northern area is close to the shore and is greatly affected by the input of land sources, with more human interference leading to poor stability of the community structure. *Nitzschia* spp. have an affinity for organic-polluted water [47] and often appear in eutrophic waters [48]. Therefore, the high-value area of *Nitzschia* spp. in the coastal waters of the study area indicated eutrophication and slightly polluted water. Overall, the water quality in the south of the investigated area was better than that in the north.

4.4. Correlation between Phytoplankton Community Structure and Environmental Factors

Overall, the phytoplankton community in the northern SCS had no significant correlation with ammonium salt, but was negatively correlated with the sum of nitrate and nitrite. In general, among the three DIN types, phytoplankton preferentially absorbed ammonium nitrogen because they require less energy than nitrate-nitrogen [49]. However, the ammonium salt content in the SCS was extremely low [50]. Phytoplankton absorb nitrate- and nitrite-nitrogen to maintain their growth and reproduction. The extensive use of nitrate- and nitrite-nitrogen leads to a decrease in the nitrate/nitrite content and an increase in the number of phytoplankton. Therefore, the number of phytoplankton was negatively correlated with the sum of nitrate and nitrite in the data [51]. The SCS is an oligotrophic sea area, which is often restricted by nitrogen. The nitrogen quota of phytoplankton with large cell volumes is large, and the absorption capacity of phytoplankton with large cell volumes for nitrogen salt is related to its minimum nitrogen quota. Therefore, in the SCS, where nitrogen is limited, small- and medium-sized phytoplankton are usually dominant.

5. Conclusions

In the present study, we analyzed the structure and characteristics of the phytoplankton community in the northern SCS during the summer of 2020. Combined with historical

data, we discussed the evolutionary trends of the phytoplankton community and the succession of dominant species. Based on the field survey and detection data, the environmental factors affecting the phytoplankton community structure in the northern SCS were analyzed, and the water quality in the sea area was evaluated. We observed that eutrophication occurred near the shore. As phytoplankton play an important role in the calculation of carbon storage, we will further analyze the change in carbon storage in the SCS and its influencing factors based on long-term data on the changes in the phytoplankton community structure in the SCS.

Author Contributions: W.C. contributed to the analysis of data, and preparation of the manuscript. J.G. contributed to drafted the manuscript. Z.X. contributed to guide the writing of manuscripts. S.Y. contributed to guide the writing of manuscripts, manuscript revision, and read and approved the submitted version. Y.Y. contributed to the identification of phytoplankton and the collection of samples. All authors have read and agreed to the published version of the manuscript.

Funding: The study was supported by the National Science Foundation of China. Data and samples were collected onboard the R/V XIANG YANG HONG 18. The open research cruise NORC2020-05 was supported by the NSFC Shiptime Sharing Project (project number: 31750001).

Data Availability Statement: Not applicable.

Acknowledgments: The crews on the research cruise are thanked for their help with data collection. We are also very grateful to the First Institute of Oceanography and the Ministry of Natural Resources for providing the nutrient data.

Conflicts of Interest: We state that there were no conflict of interest related to this study. All funding information and people who gave help during this study have been stated in the manuscripts.

Appendix A

Table A1. Species list of the phytoplankton assemblage in the northern South China Sea, during summer of 2020.

Bacillariophyta	*Chaetoceros distans* Cleve
Achnanthes brevipes Agardh	*Chaetoceros femur* Schütt
Actinocyclus octonarius Ehrenberg	*Chaetoceros hirundinellus* Qian
Actinocyclus octonarius Ehrenberg	*Chaetoceros imbricatus* Mangin
Actinoptychus hexagonus Grunow in Schmidt	*Chaetoceros indicus* Karsten
Actinoptychus senarius (Ehr.) Ehrenberg	*Chaetoceros knipowitschii* Henckel
Asterolampra marylandica Ehrenberg	*Chaetoceros lauderi* Ralfs
Asterolampra vanheurckii Brun	*Chaetoceros messanensis* Castracane
Asteromphalus cleveanus Grunow	*Chaetoceros pelagicus* Cleve
Asteromphalus elegans Greville	*Chaetoceros pendulus* Karsten
Asteromphalus flabellatus (Brébisson) Greville	*Chaetoceros peruvianus* Brightwell
Asteromphalus heptactis (Breb.) Ralfs	*Chaetoceros pseudodichaeta* Ikari
Asteromphalus rubustus Castracane	*Chaetoceros rostratus* Lauder
Asteromphalus spp.	*Chaetoceros rostratus* var. *glandazi* Mangin
Bacillaria paxillifera (Müller) Hendey	*Chaetoceros* spp.
Bacteriastrum comosum Pavillard	*Chaetoceros teres* Cleve
Bacteriastrum elongatum Cleve	*Chaetoceros tetrastichon* Cleve
Bacteriastrum furcatum Shadbolt	*Chaetoceros tortissimus* Gran
Bacteriastrum hyalinum Lauder	*Climacodium frauenfeldianum* Grunow
Bacteriastrum mediterraneum Pavillard	*Corethron criophilum* Castracane
Biddulphia sinensis Greville	*Coscinodiscus debilis* Grove
Campylosira cymbelliformis (Schmidt) Grunow ex Van Heurck	*Coscinodiscus gigas* Ehrenberg
Cerataulina bergonii Ostenfeld	*Coscinodiscus granii* Grough
Chaetoceros aequatoriale Cleve	*Coscinodiscus jonesianus* (Greville) Ostenfeld
Chaetoceros affinis Lauder	*Coscinodiscus nobilis* Grunow
Chaetoceros atlanticus Cleve	*Coscinodiscus oculus-iridis* Ehrenberg
Chaetoceros atlanticus var. *neapolitana* (Schröder) Hustedt	*Coscinodiscus* spp.
Chaetoceros atlanticus var. *skeleton* (Schütt) Hustedt	*Coscinodiscus subtilis* Ehrenberg
Chaetoceros aurivillii Cleve	*Cyclotella striata* (Kuetz.) Grunow
Chaetoceros bacteriastroides Karsten	*Chaetoceros diadema* (Ehrenberg) Gran

Table A1. *Cont.*

Chaetoceros buceros Karsten
Chaetoceros castracanei Karsten
Chaetoceros coarctatus Lauder
Chaetoceros compressus Lauder
Chaetoceros constrictus Gran
Chaetoceros dadayi Pavillard
Chaetoceros danicus Cleve
Chaetoceros debilis Cleve
Chaetoceros decipiens f. *singularis* Gran
Chaetoceros densus (Cleve) Cleve
Chaetoceros denticulatus f. *angusta* Hustedt ex Simonsen
Guinardia delicatula (Cleve) Hasle et al.
Guinardia striata (Stolterfoth) Hasle et al.
Gyrosigma balticum (Ehrenberg) Cleve
Helicotheca tamesis (Shrubsole) Ricard
Hemiaulus hauckii Grunow ex Van Heurck
Hemiaulus sinensis Greville
Hemidiscus cuneiformis var. *cuneiformis* Wallich
Lauderia annulata Cleve
Lauderia mediterranea Peragallo
Lauderia pumila Castracane
Leptocylindrus danicus Cleve
Mastogloia rostrata (Wallich) Hustedt
Meuniera membranacea (Cleve) Silva
Navicula spp.
Nitzschia longissima (Brébisson) Ralfs
Nitzschia lorenziana Grunow
Nitzschia spp.
Odontella longicruris (Greville) Hoban
Odontella mobiliensis (Bailey) Grunow
Odontella regia (Schultze) Simonsen
Odontella spp.
Paralia sulcata (Ehrenberg) Cleve
Pinnularia spp.
Planktoniella blanda Syvertsen & Hasle
Planktoniella formosa Qian & Wang
Pleurosigma acutum Norman
Proboscia alata (Brightwell) Sundström
Pseudo-nitzschia delicatissima (Cleve) Heiden et al.
Pseudo-nitzschia pungens (Grunow ex Cleve) Hasle
Pseudosolenia calcar-avis (Schultze) Sundström
Rhizosolenia alata f. *indica* (Peragallo) Ostenfeld
Rhizosolenia bergonii Peragallo
Rhizosolenia castracanei Peragallo
Rhizosolenia clevei Ostenfeld
Rhizosolenia cochlea Brun
Rhizosolenia gracillima Cleve
Rhizosolenia hyalina Ostenfeled et Schmidt
Rhizosolenia imbricata Brightwell
Rhizosolenia robusta Norman ex Ralfs
Rhizosolenia semispina Hensen
Rhizosolenia setigera Brightwell
Rhizosolenia sinensis Qian
Rhizosolenia styliformis Brightwell
Dinophysis doryphorum (Stein) Abé
Dinophysis expulsa Kofoid et Michener
Dinophysis fortii Pavillard
Dinophysis laevis Claparède & Lachmann
Dinophysis mitra (Schütt) Abé
Dinophysis ovata Claparède & Lachmann
Dinophysis oviformis Chen & Ni
Dinophysis parvula (Schütt) Balech
Dinophysis porodictyum (Stein) Abé
Dinophysis rapa (Stein) Abé
Dinophysis rotundata Claparède & Lachmann
Dinophysis schuettii Murray & Whitting
Dinophysis spp.
Dinophysis tailisuni Chen & Ni
Diploneis bombus Ehrenberg
Ditylum brightwellii (West) Grunow
Ditylum sol Grunow
Donkinia sp.
Eucampia cornuta (Cleve) Grunow
Eucampia zodiacus Ehrenberg
Eunotogramma debile Grunow in Van Heurck
Fragilaria spp.
Fragilariopsis doliolus (Wallich) Medlin & Sims
Gossleriella tropica Schütt
Rhizosolenia styliformis var. *latissima* Brightwell
Schröderella delicatula f. *schröderi* (Bergon) Sournia
Skeletonema costatum (Greville) Cleve
Stephanopyxis turris (Greville) Ralfs
Streptotheca indica Karsten
Synedra spp.
Thalassionema frauenfeldii (Grunow) Hallegraeff
Thalassionema nitzschioides Grunow
Thalassiosira leptopus (Grunow ex Van Heurck) Hasle & G. Fryxell
Thalassiosira nordenskiöldii Cleve
Thalassiosira rotula Meunier
Thalassiosira spp.
Thalassiothrix longissima Cleve et Grunow
Triceratium affine Grunow
Dinophyta
Akashiwo sanguinea (Hirasaka) Hansen & Moestrup
Alexandrium cohorticula (Balech) Balech
Alexandrium spp.
Alexandrium tamiyavanichii Balech
Amphidoma nucula Stein
Amphisolenia bidentata Schröder
Amphisolenia brevicauda Kofoid
Amphisolenia globifera Stein
Amphisolenia inflata Murray & Whitting
Amphisolenia thrinax Schütt
Amylax triacantha (Jörgensen) Sournia
Blepharocysta splendor-maris (Ehrenberg) Ehrenberg
Ceratium declinatum var. *angusticornum* Peters
Ceratocorys horrida Stein
Ceratocorys magna Kofoid
Citharistes regius Stein
Cladopyxis brachiolata Stein
Corythodinium belgicae (Meunier) F.J.R. Taylor
Corythodinium carinatum (Gaarder) F.J.R. Taylor
Corythodinium compressum (Kofoid) Taylor
Corythodinium constrictum (Stein) Taylor
Corythodinium curvicaudatum (Kofoid) F.J.R. Taylor
Corythodinium elegans (Pavillard) Taylor
Corythodinium frenguellii (Rampi) Taylor
Corythodinium tesselatum (Stein) Loeblich Jr. & Loeblich III
Dinophysis acuminata Claparède et Lachmann
Dinophysis argus (Stein) Abé
Dinophysis caudata Saville-Kent
Dinophysis cuneus (Schütt) Abé
Histioneis costata Kofoid & Michener
Histioneis cymbalaria Stein
Histioneis para Murray & Whitting
Histioneis parallela Gaarder
Histioneis pulchra Kofoid
Histioneis biremis Stein
Histioneis cleaveri Rampi
Karenia spp.
Lingulodinium polyedrum (Stein) Dodge
Neoceratium arietinum (Cleve) Gómez, Moreira & López-Garcia
Neoceratium axiale (Kofoid) Gómez, Moreira & López-Garcia
Neoceratium belone (Cleve) Gómez, Moreira & López-Garcia
Neoceratium biceps (Claparède & Lachmann) Gómez, Moreira & López-Garcia
Neoceratium boehmii (Graham et Bronikovsky)

Table A1. *Cont.*

Dinophysis uracantha Stein
Diplopsalopsis bomba (Stein ex Jorgensen) Dodge & Toriumi
Diplopsalopsis globula Abé
Dissodinium lunula Schütt
Dolichodinium lineatum (Kofoid & Michener) Kofoid & Adamson
Goniodoma polyedricum (Pouchet) Jörgensen
Goniodoma sphaericum Murray & Whitting
Gonyaulax birostris Stein
Gonyaulax brevisulcata Dangeard
Gonyaulax digitale (Pouchet) Kofoid
Gonyaulax fusiformis Graham
Gonyaulax hyalina Ostenfeld & Schmidt
Gonyaulax kofoidii Pavillard
Gonyaulax milneri (Murray & Whitting) Kofoid
Gonyaulax minuta Kofoid & Michener
Gonyaulax monacantha Pavillard
Gonyaulax monospina Rampi
Gonyaulax pacifica Kofoid
Gonyaulax polygramma Stein
Gonyaulax sphaeroidea Kofoid
Gonyaulax subulata Kofoid & Michener
Gonyaulax turbynei Murray & Whitting
Gonyaulax verior Sournia
Gymnodinium spp.
Gyrodinium dominans Hulbert
Gyrodinium fusiform
Gyrodinium spirale (Bergh) Kofoid et Swezy
Histioneis depressa Schiller
Histioneis gregoryi Böhm
Histioneis highleyi Murray & Whitting
Histioneis oxypteris Schiller
Histioneis panda Kofoid & Michener
Ornithocercus thumii (Schmidt) Kofoid & Skogsberg
Oxytoxum crassum Schiller
Oxytoxum curvatum (Kofoid) Kofoid
Oxytoxum elongatum Wood
Oxytoxum laticeps Schiller
Oxytoxum milneri Murray & Whitting
Oxytoxum mitra Stein
Oxytoxum mucronatum Hope
Oxytoxum parvum Schiller
Oxytoxum sceptrum (Stein) Schröder
Oxytoxum scolopax Stein
Oxytoxum sphaeroideum Stein
Oxytoxum subulatum Kofoid
Oxytoxum turbo Kofoid
Oxytoxum variabile Schiller
Palaeophalacroma unicinctum Schiller
Palaeophalacroma verrucosum Schiller
Podolampas bipes Stein
Podolampas palmipes Stein
Podolampas spinifera Okamura
Pronoctiluca pelagica Fabre-Domerqne
Prorocentrum compressum (Ostenfeld) Abé
Prorocentrum dentatum Stein
Prorocentrum lenticulatum (Matzenauer) Taylor
Prorocentrum micans Ehrenberg
Prorocentrum minimun (Pavillard) Schiller
Prorocentrum rostratum Stein
Prorocentrum sigmoides Böhm
Prorocentrum spp.
Prorocentrum triestinum Schiller
Protoceratium areolatum Kofoid
Protoceratium reticulatum (Claparède & Lachmann) Butschli
Protoceratium spinulosum (Murray & Whitting) Schiller
Protoperidinium acanthophorum (Balech) Balech
Protoperidinium achromaticum (Levander) Balech
Neoceratium carriense (Gourret) Gómez, Moreira & López-Garcia
Neoceratium deflexum (Kofoid) Gómez, Moreira & López-Garcia
Neoceratium ehrenbergii (Kofoid)
Neoceratium extensum (Gourret) Gómez, Moreira & López-Garcia
Neoceratium falcatum (Kofoid) Gómez, Moreira & López-Garcia
Neoceratium furca (Ehrenberg) Gómez, Moreira & López-Garcia
Neoceratium furca var. *nannofurca* (Jörgensen) Yang, Li & Dong
Neoceratium fusus (Ehrenberg) Gómez, Moreira & López-Garcia
Neoceratium gravidum (Gourret) Gómez, Moreira & López-Garcia
Neoceratium hexacanthum (Gourret) Gómez, Moreira & López-Garcia
Neoceratium hircus (Schröder) Gómez, Moreira & López-Garcia
Neoceratium horridum (Gran) Gómez, Moreira & López-Garcia
Neoceratium karstenii (Pavillard) Gómez, Moreira & López-Garcia
Neoceratium lineatum (Ehrenberg) Gómez, Moreira & López-Garcia
Neoceratium macroceros (Ehrenberg) Gómez, Moreira & López-Garcia
Neoceratium macroceros var. *gallicum* (Kofoid) Yang, Li & Dong
Neoceratium massiliense (Gourret) Gómez, Moreira & López-Garcia
Neoceratium minutum (Jørgensen) Gómez, Moreira & López-Garcia
Neoceratium pentagonum (Gourret) Gómez, Moreira & López-Garcia
Neoceratium praeolongum (Lemmermann) Gómez, Moreira & López-Garcia
Neoceratium ranipes (Cleve) Gómez, Moreira & López-Garcia
Neoceratium seta (Ehrenberg) Yang & Li
Neoceratium sumatranum (Karsten) Yang & Li
Neoceratium tenue (Ostenfeld & Schmidt) Gómez, Moreira & López-Garcia
Neoceratium teres (Kofoid) Gómez, Moreira & López-Garcia
Neoceratium trichoceros (Ehrenberg) Gómez, Moreira & López-Garcia
Neoceratium tripos (O.F. Müller) Gómez, Moreira & López-Garcia
Noctiluca scintillans (Macartney) Ehrenberg
Ornithocercus heteroporus Kofoid
Ornithocercus magnificus Stein
Ornithocercus quadratus v. *quadratus* Schütt
Ornithocercus skogsbergii Abé
Protoperidinium acutum (Karsten) Balech
Protoperidinium asymmetricum (Abé) Balech
Protoperidinium breve Paulsen
Protoperidinium curtipes (Jörgensen) Balech
Protoperidinium depressum (Bailey) Balech
Protoperidinium divergens (Ehrenberg) Balech
Protoperidinium elegans (Cleve) Balech
Protoperidinium exageratum Balech
Protoperidinium globulus (Stein) Balech
Protoperidinium grande (Kofoid) Balech
Protoperidinium heterocanthum (Dangeard) Balech
Protoperidinium latispinum (Mangin) Balech
Protoperidinium leonis (Pavillard) Balech
Protoperidinium melo (Balech) Balech
Protoperidinium obtusum (Karsten) Parke & Dodge
Protoperidinium orientale (Matzenauer) Balech
Protoperidinium parvum Abé
Protoperidinium porosum Balech
Protoperidinium pyriforme (Paulsen) Balech
Protoperidinium quarnerense (B. Schröder) Balech
Protoperidinium rhombiforme (Abé) Balech
Protoperidinium schilleri (Paulsen) Balech
Protoperidinium steinii (Jörgensen) Balech
Protoperidinium tenuissimum (Kofoid) Balech
Protoperidinium tuba (Schiller) Balech
Protoperidinium variegatum (Peters) Balech
Protoperidinium venustum (Matzenauer) Balech
Pyrocystis lunula (Schütt) Schütt
Pyrophacus steinii (Schiller) Wall & Dale
Schuettiella mitra (Schütt) Balech
Scrippsiella trochoidea (Stein) Loeblich III
Triposolenia bicornis Kofoid
Chrysophyta
Dictyocha fibula Ehrenberg
Dictyocha speculum Ehrenberg

References

1. Pan, H.; Li, A.; Cui, Z.; Ding, D.; Qu, K.; Zheng, Y.; Lu, L.; Jiang, T.; Jiang, T. A comparative study of phytoplankton community structure and biomass determined by HPLC-CHEMTAX and microscopic methods during summer and autumn in the central Bohai Sea, China. *Mar. Pollut. Bull.* **2020**, *155*, 111172. [CrossRef] [PubMed]
2. Jia, J.; Gao, Y.; Zhou, F.; Shi, K.; Johnes, P.J.; Dungait, J.A.J.; Ma, M.; Lu, Y. Identifying the main drivers of change of phytoplankton community structure and gross primary productivity in a river-lake system. *J. Hydrol.* **2020**, *583*, 124633. [CrossRef]
3. McCollin, T.; Shanks, A.M.; Dunn, J. Changes in zooplankton abundance and diversity after ballast water exchange in regional seas. *Mar. Pollut. Bull.* **2008**, *56*, 834–844. [CrossRef] [PubMed]
4. Righetti, D.; Vogt, M.; Gruber, N.; Psomas, A.; Zimmermann, E.N. Global pattern of phytoplankton diversity driven by temperature and environmental variability. *Sci. Adv.* **2019**, *5*, eaau6253. [CrossRef] [PubMed]
5. Dunne, J.P. Fall and rise of the phytoplankton. *Nat. Clim. Change* **2022**, *12*, 708–709. [CrossRef]
6. Toseland, A.; Daines, S.J.; Clark, J.R.; Kirkham, A.; Strauss, J.; Uhlig, C.; Lenton, T.M.; Valentin, K.; Pearson, G.A.; Moulton, V.; et al. The impact of temperature on marine phytoplankton resource allocation and metabolism. *Nat. Clim. Change* **2013**, *3*, 979–984. [CrossRef]
7. Doney, S.C. Plankton in a warmer world. *Nature* **2006**, *444*, 695–696. [CrossRef] [PubMed]
8. Hu, J.Y.; Wang, X.H. Progress on upwelling studies in the China seas. *Rev. Geophys.* **2016**, *54*, 653–673. [CrossRef]
9. Li, D.; Chou, W.; Shih, Y.; Chen, G.; Chang, Y.; Chow, C.H.; Lin, T.; Hung, C. Elevated particulate organic carbon export flux induced by internal waves in the oligotrophic northern South China Sea. *Sci. Rep.* **2018**, *8*, 2042. [CrossRef] [PubMed]
10. El-Sherif, Z.; Mikhail, S.K. Phytoplankton dynamics in the southwestern part of Abu Qir Bay, Alexandria, Egypt. Egypt. *J. Aquat. Biol. Fish* **2003**, *7*, 219–239.
11. Alprol, A.E.; Ashour, M.; Mansour, A.T.; Alzahrani, O.M.; Mahmoud, S.F.; Gharib, S.M. Assessment of Water Quality and Phytoplankton Structure of Eight Alexandria Beaches, Southeastern Mediterranean Sea, Egypt. *J. Mar. Sci. Eng.* **2021**, *9*, 1328. [CrossRef]
12. Alprol, A.E.; Heneash, A.M.M.; Ashour, M.; El-Kafrawy, S.; Soliman, A.M. Chemical assessment of water quality, heavy metals, and the distribution of zooplankton communities, based on field and GIS data in the drains of Burullus Lake, Egypt. *Arab. J. Geosci.* **2022**, *15*, 1511. [CrossRef]
13. Utermöhl, H. Zur Vervollkommung der quantitativen Phytoplankton-Methodik. *Mitt. Inter. Verein. Lim.* **1958**, *9*, 1–38.
14. Sun, J.; Liu, D.Y.; Qian, S.B. A quantitative research and analysis method for marine phytoplankton: An introduction to Utermöhl method and its modification. *J. Oceanogr. Huanghai Bohai Seas* **2002**, *20*, 105–112.
15. Niu, H.Y.; Chen, C.; Han, B.P. Quality and reliability of quantifying phytoplankton abundance and biomass data based upon the concentrated water sample method. *J. Lake Sci.* **2015**, *05*, 776–782.
16. Yang, S.M.; Dong, S.G. *Atlas of Common Planktonic Diatoms in China Sea Area*; Ocean University of China Press: Qingdao, China, 2006; pp. 1–267.
17. Yang, S.M.; Li, R.X.; Dong, S.G. *Dinoflagellates I (Prorocentrales, Dinophysiaoes) in Chinese Waters*; Ocean Press: Beijing, China, 2014; pp. 1–156.
18. Yang, S.M.; Li, R.X.; Dong, S.G. *Dinoflagellates II (Goneaulacales) in Chinese Waters*; Ocean Press: Beijing, China, 2016; pp. 1–248.
19. Yang, S.M.; Li, R.X.; Dong, S.G. *Dinoflagellates III (Peridiniales) in Chinese Waters*; Ocean Press: Beijing, China, 2019; pp. 1–211.
20. Shannon, C.E.; Weaver, W. *The Mathematical Theory of Communication*; University of Illinois Press: Urbana, IL, USA, 1949; pp. 1–125.
21. Pielou, E.G. An introduction to mathematical ecology. *J. Ecol.* **1970**, *58*, 1–286.
22. Lampitt, R.S.; Wishner, K.F.; Turley, C.M.; Angel, M.V. Marine snow studies in the Northeast Atlantic Ocean: Distribution, composition and role as a food source for migrating plankton. *Mar. Biol.* **1993**, *116*, 689–702. [CrossRef]
23. Taylor, F. Scanning electron microscopy of thecae of the dinoflagellate genus ornithocercus. *J. Phycol.* **2010**, *7*, 249–258. [CrossRef]
24. Sha, L.B.; Huang, Y.; Wang, L. Paleoenvironmental significance of thalassionema nitzschioides and its varieties of core 17940 in the South China Sea during the latest pleistocene. *J. Meteorol. Enviroment* **2008**, *24*, 5.
25. Xu, Z.T.; Li, S.Y.; Hu, J.T.; Wang, S.Y.; Wang, B.; Guo, M.X. Summer phytoplankton responses to upwelling and river plume in northern South China Sea. *J. Trop. Oceanogr.* **2018**, *37*, 12.
26. Shu, Y.Q.; Wang, Q.; Zu, T.T. Progress on shelf and slope circulation in the northern South China Sea. *Sci. Sin. (Terrae)* **2018**, *48*, 12. [CrossRef]
27. Xiao, W.; Laws, E.A.; Xie, Y.; Wang, L.; Huang, B. Responses of marine phytoplankton communities to environmental changes: New insights from a niche classification scheme. *Water Res.* **2019**, *166*, 115070. [CrossRef] [PubMed]
28. Zhang, Z.; Zhou, M.; Zhong, Y.; Zhang, G.; Jiang, S.; Gao, Y.; Zhang, R.; Smith, W.O., Jr. Spatial variations of phytoplankton biomass controlled by river plume dynamics over the lower changjiang estuary and adjacent shelf based on high-resolution observations. *Front. Mar. Sci.* **2020**, *7*, 587539. [CrossRef]
29. Zheng, M.L.; Li, M.M.; Xie, L.L.; Hong, Y.B.; He, Y.K.; Zong, X.L. Observation and analysis of winter hydrological characteristics of Northwest continental shelf of South China Sea in 2012. *Oceanol. Et Limnol. Sin.* **2018**, *49*, 12.
30. Murrell, M.C.; Lores, E.M. Phytoplankton and zooplankton seasonal dynamics in a subtropical estuary: Importance of cyanobacteria. *J. Plank. Res.* **2004**, *26*, 371–382. [CrossRef]
31. Glibert, P.; Burkholder, J.; Kana, T.; Alexander, J.; Skelton, H.; Shilling, C. Grazing by karenia brevis on synechococcus enhances its growth rate and may help to sustain blooms. *Aquat. Microb. Ecol.* **2009**, *55*, 17–30. [CrossRef]

32. Ou, L.J.; Wang, D.; Huang, B.Q.; Hong, H.S.; Qi, Y.Z.; Lu, S.H. Comparative study of phosphorus strategies of three typical harmful algae in Chinese coastal waters. *J. Plankton Res.* **2008**, *30*, 1007–1017. [CrossRef]
33. Ou, L.J.; Huang, B.Q.; Hong, H.S.; Qi, Y.Z.; Lu, S.H. Comparative alkaline phosphatase characteristics of the algal bloom dinoflagellates *Prorocentrum donghaiense* and *Alexandrium catenella*, and the diatom *Skeletonema costatum*. *J. Phycol.* **2010**, *46*, 260–265. [CrossRef]
34. Coble, G.P. Marine Optical Biogeochemistry: The Chemistry of Ocean Color. *Chem. Rev.* **2007**, *107*, 402–418. [CrossRef]
35. Xue, B.; Sun, J.; Li, T.T. Phytoplankton community structure of northern South China Sea in summer of 2014. *Acta Oceanol. Sin.* **2016**, *38*, 54–65.
36. Zhuang, W.; Hu, J.Y.; He, Z.G.; Zeng, G.N.; Chen, Z.Z. An analysis on surface temperature and salinity from southern Taiwan Strait to ZhuJiang River Estuary during July-August. *J. Trop. Oceanogr.* **2003**, *22*, 68–76.
37. Gan, J.P.; Lu, Z.M.; Cheung, A.; Dai, M.H.; Liang, L.L.; Harrison, P.J.; Zhao, X.Z. Assessing ecosystem response to phosphorus and nitrogen limitation in the Pearl River plume using the Regional Ocean Modeling System (ROMS). *J. Geophys. Res. Ocean.* **2014**, *119*, 8858–8877. [CrossRef]
38. Van Mooy, B.A.; Fredricks, H.F.; Pedler, B.E.; Dyhrman, S.T.; Karl, D.M.; Koblízek, M.; Lomas, M.W.; Mincer, T.J.; Moore, L.R.; Moutin, T.; et al. Phytoplankton in the ocean use non-phosphorus lipids in response to phosphorus scarcity. *Nature* **2009**, *458*, 69–72. [CrossRef] [PubMed]
39. Zhou, Z.P.; Zhou, X.J.; Song, Y.Q. Effects of nitrogen and phosphorus supplies on the growth and intracellular composition for Chaetoceros gracilis. *J. Aquac.* **2020**, *41*, 24–29.
40. Li, L.; Chen, Z.Z.; Huang, Z.R.; Xu, Y.W. Net-collected phytoplankton communitystructure in relation to environmental factors in the continental shelf of the northern South China Sea in spring 2015. *J. Mar. Sci.* **2019**, *3*, 86–96.
41. Li, D.R.; Dai, X.F.; Lu, D.D.; Xia, P. Community structure of net-phytoplankton in the northwest South China Sea in the summer of 2012. *J. Mar. Sci.* **2014**, *32*, 87–96.
42. Ma, W.; Sun, J.; Xue, B.; Dai, M.H.; Hu, J.Y. Study on phytoplankton community structure in northern South China Sea in autumn 2010. *J. Mar. Sci.* **2016**, *38*, 43–53.
43. Li, X.; Sun, J.; Tian, W.; Wang, M. Phytoplankton communities in the northern South China Sea in summer 2009. *J. Mar. Sci.* **2012**, *36*, 33–39.
44. Ling, J.; Dong, J.D.; Zhang, Y.Y.; Wang, Y.S.; Deng, C.; Lin, L.; Chen, L.; Li, T.; Long, L.J. Structure characteristics of phytoplankton community in Northern South China Sea in the summer of 2008. *J. Biol.* **2012**, *29*, 42–46.
45. Ke, Z.X.; Huang, L.M.; Tan, Y.H.; Yin, J.Q. Species composition and abundance of phytoplankton in the northern South China Sea in summer 2007. *J. Trop. Oceanogr.* **2011**, *30*, 131–143.
46. Le, F.F.; Sun, J.; Ning, X.R.; Song, S.Q.; Cai, Y.M.; Liu, C.G. Phytoplankton in the northern South China Sea in summer 2004. *Oceanol. Limnol. Sin.* **2006**, *03*, 238–248.
47. Dam, H.V.; Mertens, A.; Sinkeldam, J. A coded checklist and ecological indicator values of freshwater diatoms from The Netherlands. *Neth. J. Aquat. Ecol.* **1994**, *28*, 117–133. [CrossRef]
48. Tudesque, L.; Rimet, F.; Ector, L. A new taxon of the section *Nitzschiae Lanceolatae* Grunow: *Nitzschia costei* sp. nov. Compared to *N. fonticola* Grunow, *N. macedonica* Hustedt, *N. tropica* Hustedt and related species. *Diatom Res.* **2008**, *23*, 483–501. [CrossRef]
49. Mukherjee, R.; Kumar, S.; Muduli, P.R. Spatial variation of nitrogen uptake rates in the largest brackish water lagoon of Asia (Chilika, India). *Estuar. Coast. Shelf Sci.* **2019**, *216*, 87–97. [CrossRef]
50. Li, J.J.; Tan, Y.H.; Zhou, L.B.; Jiang, X.; Zhao, C.Y. Effects of nutrients on phytoplankton growth in the oligotrophic waters of north-eastern South China Sea. *Mar. Sci. Bull.* **2016**, *35*, 9.
51. Jiang, Z.B.; Chen, J.F.; Zhou, F.S.; Shou, L.; Chen, Q.Z.; Tao, B.Y.; Yan, X.J.; Wang, K. Controlling factors of summer phytoplankton community in the Changjiang (Yangtze River) Estuary and adjacent East China Sea shelf. *Cont. Shelf Res.* **2015**, *101*, 71–84. [CrossRef]